Journal of Sound and Vibration (1998) **214**(2), 201–212
Article No. sv971541

EFFECT OF CRACK DEPTH ON THE NATURAL FREQUENCY OF A PRESTRESSED FIXED–FIXED BEAM

S. Masoud, M. A. Jarrah and M. Al-Maamory

Mechanical Engineering Department, Jordan University of Science and Technology, Irbid, Jordan

(*Received* 24 *July* 1997)

The effect of crack depth on the transverse vibrational characteristics of a prestressed fixed–fixed beam is investigated. The natural frequency of the system is obtained by modal analysis. The coupling effect between the crack depth and the axial load on the natural frequency of the system is investigated. Also, experimental work verifies the results of the theoretical analysis. The study shows that there is a significant coupling between the axial load and the crack depth, and this coupling effect is directly proportional to the crack depth as well as the axial load. Therefore, the problem of a prestressed cracked beam cannot be treated as a superposition of two separate effects (crack plus axial load) to find the natural frequency of the system.

1. INTRODUCTION

Crack development, propagation, and detection have been extensively investigated over the past few decades. The effect of cracks on the dynamic behaviour of beams has received much attention because of its importance in mechanical and civil engineering applications. The problem of identifying cracks in civil engineering applications such as highway and railway bridges is of great interest [1]. The existence of a crack in a structural member introduces local flexibility, and consequently affects the dynamic behaviour of the cracked member. Chondros and Dimarogonas [2] studied the effect of the crack depth on the dynamic behaviour of a cantilevered beam. They showed that increasing the crack depth reduces the natural frequency of the beam. Free bending motion of a uniform Bernoulli–Euler beam containing one or more pairs of symmetric cracks was studied by Cristides and Barr [3]. Dannanh and Farghaly [4] developed analytical tools to study the effect of transverse open cracks on the vibratory response of stationary shafts carrying masses and mounted on elastic supports. In a combined theoretical and experimental work, Papadopoulos and Dimarogonas [5] studied the coupling between bending and longitudinal vibration of a stationary cracked shaft with an open crack. In their work, Papadopoulos and Dimarogonas concluded that the coupling effect between the bending and the longitudinal vibration is relatively weak. Rizos *et al*. [6] studied the flexural vibration of a cracked cantilever beam with a rectangular cross-section. They developed analytical relations that relate the vibration modes to the crack location and depth. Narkis [7] modelled the crack by an equivalent spring connecting the two segments of the cracked beam. An eigensystem was obtained to relate the natural frequencies of the beam to the crack location and depth. Haisty and Springer [8] used a finite element approach and developed a general beam element containing an open double-sided crack which can be

0022–460X/98/270201 + 12 $30.00/0

used to model the damage in complex structures. Gounaris and Dimarogonas [9] used a finite element method to study a surface crack on the beam section and developed an element that describes the local flexibility of the crack. Also, a finite element approach was used by Sekhar and Prabhu [10] to study the free and forced vibration of a simply supported shaft with a transverse crack. Chondros and Dimarogonas [11] used energy methods to estimate the changes in natural frequencies and modes of cracked structure for a prescribed crack geometry. Ostachowicz and Krawczuk [12] showed that a crack can be identified by analysing the structure's forced response. Pandey and Biswas [13] concluded that the evaluation of the changes in the flexibility matrix of a structure can be used for identifying the presence of the damage and locating the damage. The approximate Galerkin solution of a one-dimensional cracked beam developed by Christides and Barr [3] was used by Shen and Pierre [14] to study the effects of symmetric cracks on the modes of free vibration of beams upon bending, and the results were compared to finite element competence.

The influence of an axial compressive load on the natural frequencies and mode shapes of a uniform single-span beam was studied by Bokaian [15] using different combinations of boundary conditions. He found that the natural frequency is inversely proportional to the compressive load. Tensile loading was shown to produce an opposite effect on the frequency in a study made by Currie and Gleghorn [16]. They used analytical tools to predict the fundamental natural frequency of a uniform beam carried by a flexible support under tensile loading.

In all previous studies, the effects of both the crack and the load on the natural frequency of a beam were studied separately. None of these studies showed the behaviour of the natural frequency of a beam under simultaneous application of a crack and an axial load. In the present work the effect of prestress on the natural frequencies of a symmetrically cracked fixed–fixed beam is investigated with a stress on the coupling between the crack depth and the axial load. The modal analysis approach is used to formulate the corresponding eigenvalue problem. The effect of two parameters on the dynamic behaviour of the problem under consideration is investigated. These two parameters are the depth of the crack, and the prestress including both tensile and compressive. Experimental work was carried out to validate the theoretical model. Several fixed–fixed beams with different crack depths were tested under a wide range of prestress values for each specimen.

2. MATHEMATICAL MODELLING

The physical system under consideration consists of an axially loaded fixed–fixed beam with symmetrical double-sided crack. The beam has a uniform rectangular cross-section, and the crack is located at the middle of the beam as shown in Figure 1. The governing equation of flexural vibration for a uniform cross-sectional Bernoulli–Euler beam loaded in the axial direction is

$$EI\,\partial^4 y/\partial x^4 + P\,\partial^2 y/\partial x^2 + \rho A\,\partial^2 y/\partial t^2 = 0. \tag{1}$$

(A list of nomenclature is given in the Appendix.) For harmonic motion, the non-dimensional form of this equation is

$$\mathrm{d}^4 Y(\eta)/\mathrm{d}\eta^4 + U\,\mathrm{d}^2 Y(\eta)/\mathrm{d}\eta^2 - \beta^2 Y(\eta) = 0, \tag{2}$$

where

$$U = PL^2/EI, \qquad \beta = \omega\sqrt{\rho AL^4/EI} \qquad \text{and} \qquad \eta = x/L. \tag{3}$$

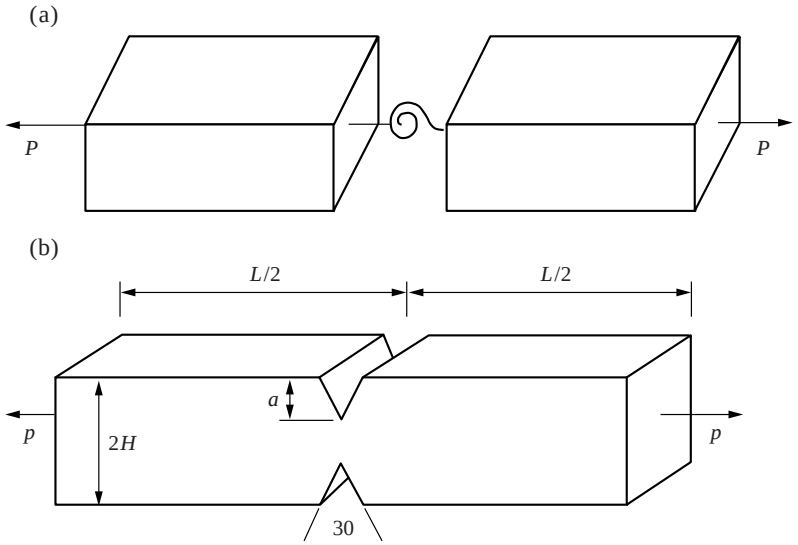

Figure 1. Axially loaded fixed–fixed beam with double-sided symmetrical cracks. (a) Mathematical model; (b) experimental model.

This equation is not valid near the crack. However, due to the localized crack effect, i.e., the crack effect is significant in the immediate crack neighbourhood only, the cracked beam can be simulated as two uniform beams joined together by a torsional spring at the crack location [7], as shown in Figure 1(b). The local flexibility of symmetrical double-sided cracks can be computed from the strain energy function. The non-dimensional flexibility is given as a function of the ratio between the crack depth and the beam thickness D, [7] by

$$\Theta = 6\pi D^2(H/L)(0{\cdot}5033 - 0{\cdot}9022D + 3{\cdot}412D^2 - 3{\cdot}181D^3 + 5{\cdot}793D^4). \tag{4}$$

The solution of equation (2) gives the modes of flexural vibration for the beam parts. The modes of vibration of the left part (Y_1) and the right part (Y_2) beam are, respectively,

$$Y_1(\eta) = C_1 \sin(\lambda_I\eta) + C_2 \cos(\lambda_I\eta) + C_3 \sinh(\lambda_R\eta) + C_4 \cosh(\lambda_R\eta), \qquad 0 \leqslant \eta \leqslant 1/2,$$

$$Y_2(\eta) = C_5 \sin(\lambda_I\eta) + C_6 \cos(\lambda_I\eta) + C_7 \sinh(\lambda_R\eta) + C_8 \cosh(\lambda_R\eta), \qquad 1/2 \leqslant \eta \leqslant 1, \tag{5}$$

where

$$\lambda_R = \sqrt{(-U + \sqrt{U^2 + 4\beta^2})/2}, \qquad \lambda_I = \sqrt{(U + \sqrt{U^2 + 4\beta^2})/2}, \tag{6}$$

and C_i, $i = 1, 2, \ldots, 8$ are constants to be determined from the boundary conditions of the beam.

The boundary conditions for the two beam parts are

$$Y_1(\eta)|_{\eta=0} = 0, \qquad Y_1'(\eta)|_{\eta=0} = 0, \qquad Y_2(\eta)|_{\eta=1} = 0, \qquad Y_2'(\eta)|_{\eta=1} = 0. \tag{7}$$

The continuity between the modes to the left and to the right of the crack should be satisfied. This implies the following conditions at the crack:

$$Y_1(\eta)|_{\eta=1/2} = Y_2(\eta)|_{\eta=1/2}, \qquad Y_1''(\eta)|_{\eta=1/2} = Y_2''(\eta)|_{\eta=1/2},$$

$$Y_1'''(\eta)|_{\eta=1/2} = -Y_2'''(\eta)|_{\eta=1/2}, \tag{8}$$

Also, the slopes of the two parts at the crack are related by the following compatibility condition:

$$Y_2'(\eta)|_{\eta=1/2} - Y_1'(\eta)|_{\eta=1/2} = \Theta\, Y_2''(\eta)|_{\eta=1/2}. \tag{9}$$

Substituting the modes equations (5) and (6) in the above boundary conditions (equations (7)–(9)) yields a set of algebraic equations of the form

$$[\mathbf{A}]\{\mathbf{C}_i\} = \{\mathbf{0}\} \qquad i = 1, 2, \ldots, 8. \tag{10}$$

The non-dimensional natural frequency (β) of the system is found by assuming a value for non-dimensional load (U) and crack depth (D), and then the determinant of the matrix [**A**] is set to be zero.

From the previous discussion, it can be seen that the value of the crack depth (D) and the applied load (U) govern the eigenvalues of the system. Thus, it can be seen that the natural frequency of an axially loaded cracked beam (β_{DP}) is a function of the crack depth and the axial load. In order to show clearly the coupling between crack depth and axial load in the natural frequency equation, a two-dimensional Taylor's series expansion is used:

$$\beta_{DP}(D, P) = \beta(D, P)|_{D=0,P=0} + \frac{\partial\beta}{\partial D|_{D=0.P=0}}\Delta D + \frac{\partial\beta}{\partial P|_{D=0,P=0}}\Delta P + \frac{\partial^2\beta}{\partial D\,\partial P|_{D=0,P=0}}\Delta D\,\Delta P + \frac{1}{2}\frac{\partial^2\beta}{\partial D^2|_{D=0,P=0}}\Delta D^2 + \cdots. \tag{11}$$

Equation (11) can be divided into three terms as follows. The first one measures the natural frequency for a cracked beam only (i.e., the axial load P is equal to zero):

$$\beta_D(D) = \beta_0 + \frac{\partial\beta}{\partial D|_{D=0,P=0}}\Delta D + \frac{1}{2}\frac{\partial^2\beta}{\partial D^2|_{D=0,P=0}}\Delta D^2 + \cdots. \tag{12}$$

The second term measures the natural frequency for the only axially loaded beam (i.e., the crack depth ratio D is equal to zero):

$$\beta_P(P) = \beta_0 + \frac{\partial\beta}{\partial P|_{D=0,P=0}}\Delta P + \frac{1}{2}\frac{\partial^2\beta}{\partial P^2|_{D=0,P=0}}\Delta P^2 + \cdots. \tag{13}$$

The last term measures the coupling effect between the crack depth and the axial load on the natural frequency of the system:

$$\beta_{co}(D, P) = \frac{\partial^2\beta}{\partial D\,\partial P|_{D=0,P=0}}\Delta D\,\Delta P + \cdots, \qquad \text{where} \qquad \beta_0 = \beta(D, P)|_{D=0,P=0}, \tag{14, 15}$$

which is the frequency of a uniform unloaded uncracked beam. Substituting equations (12)–(15) into equation (11) yields

$$\beta_{DP} = \beta_D + \beta_P - \beta_0 + \beta_{co}. \tag{16}$$

Equation (16) is used to show the significance of the coupling term β_{co} and its effect on the natural frequency of the system. In other words, if β_{co} is found to be relatively small, one can conclude that the cracked–loaded beam can be studied by a simple superposition procedure that separates the effect of the crack from that of the load. On the other hand, if β_{co} is found to be significant, the analysis procedure cannot be performed by superposition, and instead, one should take into consideration the simultaneous application of the crack and the load.

3. EXPERIMENTAL ANALYSIS

3.1. TEST BEAM

The test specimens are made of SAE 1010 cold worked steel with the following properties: 393 MPa yield strength, 655 MPa ultimate tensile strength, and a density of 7633·9 kg/m^3. The test beams have 10 $\times$ 10 mm square cross-section and 200 mm length. The crack at the mid-span of the beam is simulated by 30° triangular cuts, as shown in Figure 1. Different crack depths between 0·0 and 2·5 mm were taken. These cuts were made by milling, where a special cutting tool with a very thin edge was used.

3.2. TEST SET-UP

A piezoelectric accelerometers, Brüel & Kjaer (B&K) type 4390, were used to measure the vibration signal for the fixed–fixed beam under consideration. This signal was pre-amplified by a three channel amplifier, and pre-filtered by a low pass filter with a cut-off frequency of 3000 Hz. Two channels were connected to two accelerometers, one fixed on the beam, and the second fixed on the beam support. A third channel was connected to the impact hammer. These channels were connected to a high speed 12 bit A/D data acquisition board attached to a 486 D $\times$ 2 PC. Data reduction software using FFT was used to obtain the frequency response of the beam, and hence the natural frequencies of the system.

4. RESULTS AND DISCUSSION

A mathematical model of an axially loaded fixed–fixed cracked beam has been presented. A schematic diagram of the problem under consideration is shown in Figure 1. The existence of a crack in a beam increases the local flexibility of the beam. The increase in the local flexibility is equivalent to lowering the local bending stiffness of the beam at the crack location. The change in the natural frequency ($\Delta\beta_D$) of the first three modes versus the crack depth (D) of an unloaded fixed–fixed cracked beam is shown in Figure 2. In this figure, it can be seen that the crack affects the first and the third modes only. The second mode is insensitive to the crack, because the crack is located at the node of the second mode. This result is in full agreement with the work done by Shen and Pierre [14]. Figure 3 was plotted to check for the insensitivity of the second natural frequency to the crack for a loaded beam. In this figure, the change in the second natural frequency ($\Delta\beta_{DP}$) is plotted versus the load for different values of crack depth. From the same figure, it can be concluded that the second frequency of a cracked–loaded beam is independent of the crack depth. Therefore, only the first and the third natural frequencies are exhibited in the present work.

The change in the first natural frequency for a prestressed fixed–fixed cracked beam ($\Delta\beta_{DP}$) versus the axial load (U) is plotted in Figure 4(a) for different values of the crack depth. This figure shows that the first natural frequency of the system under consideration is increased for tensile loading ($\Delta\beta_{DP}$ is positive), and it is decreased for compressive loading ($\Delta\beta_{DP}$ is negative). The above relation between the system frequency and the load is found to be true for cracked and uncracked beams. On the other hand, introducing a crack in the beam always reduces the frequency for an unloaded beam or a beam loaded by tension. The same thing is found for the case of compressive loading, but at a certain compression load the first natural frequency is not sensitive to the crack depth, (i.e., the reduction in the first natural frequency is constant for any value of D at this load; see Figure 4(a)). The lack of sensitivity at this point can be seen from Figure 5(a). In this figure the gradient of the change in the first natural frequency ($\Delta\beta_{DP}$) with respect to crack depth (D)

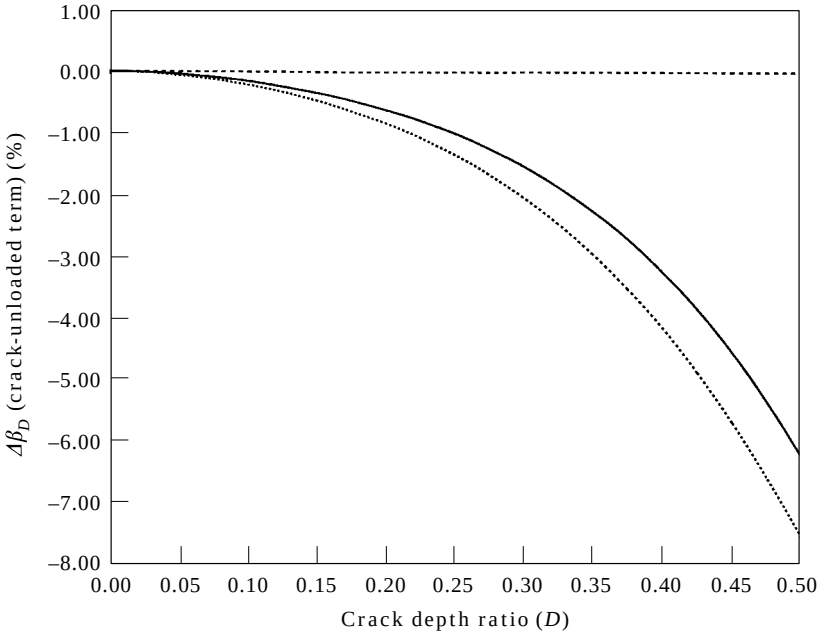

Figure 2. Percentage change in the natural frequencies of the system versus crack depth for unloaded beam. ——, First mode; – – –, second mode; · · · · , third mode.

$(\partial \Delta\beta_{DP}/\partial D|_{P\text{-const.}})$ is plotted versus the axial load for different crack depths. This figure shows that at $U_1 \approx 17{\cdot}92$ $\partial \Delta\beta_{DP}/\partial D|_{P\text{-const.}}$ is zero for any value of D. Also, from Figure 5(a) it can be seen that for a tensile load or a compressive load less than U_1, $\partial \Delta\beta_{DP}/\partial D|_{P\text{-const.}}$ is negative. This means that increasing the crack depth reduces the natural frequency; this result is clearly shown in Figure 4(a). On the other hand, if the compressive load is higher

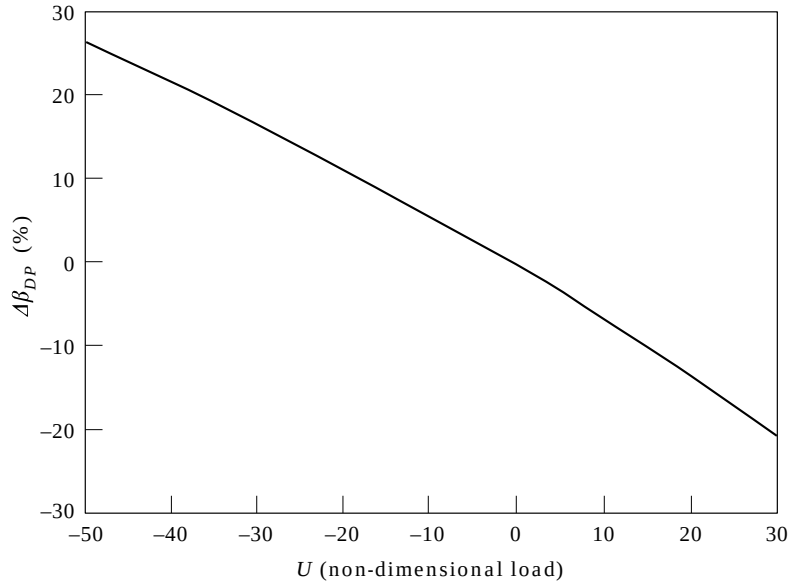

Figure 3. Percentage change in the second natural frequency versus axial load (independent of crack depth).

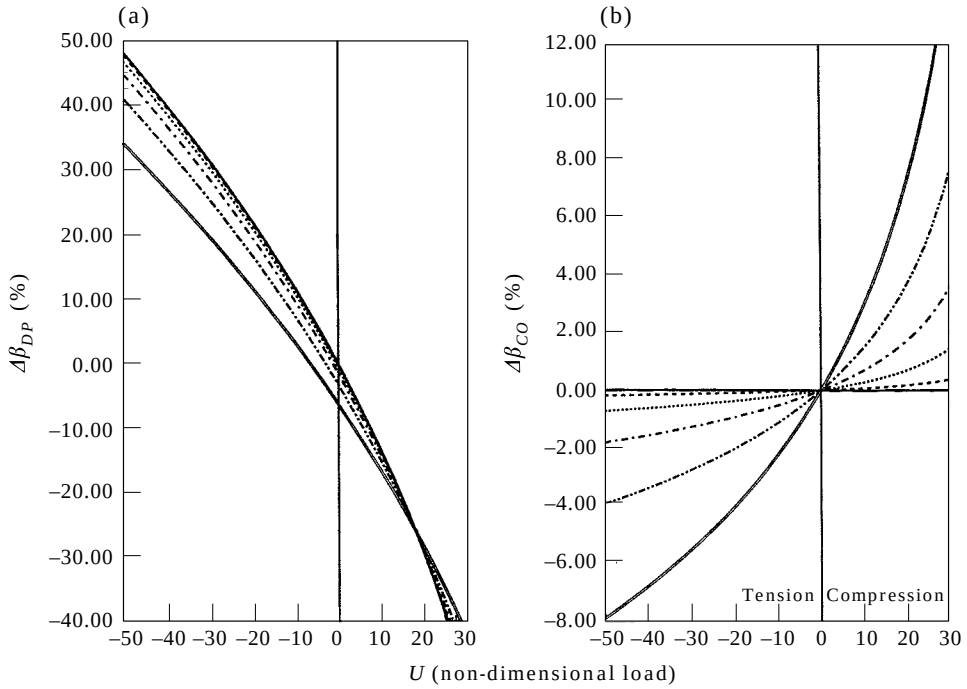

Figure 4. Percentage change in the first natural frequency versus axial load for several crack depths. (a) Crack–loaded term; (b) crack–loaded coupling term. Crack depth (D): ——, 0; – – –, 0·1; · · · ·, 0·2; –·–·–, 0·3; –··–··–, 0·4; = = , 0·5.

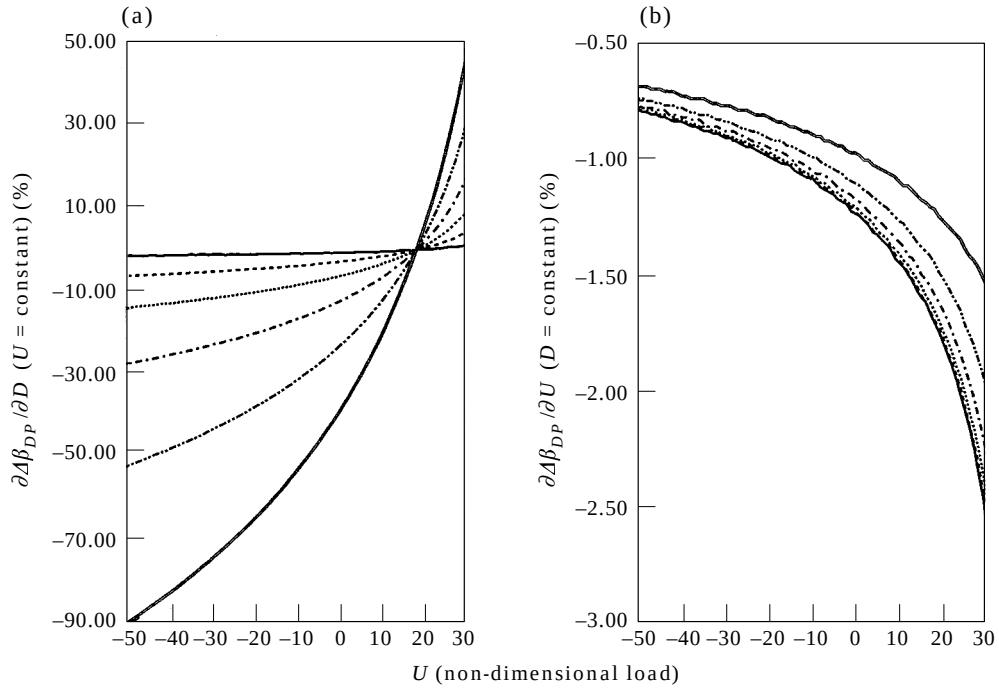

Figure 5. Gradients of the percentage change in the first natural frequency versus axial load for several crack depths. (a) With respect to crack depth (D); (b) with respect to axial load (U). Key as Figure 4.

than U_1 the gradient is positive, which means that increasing the crack depth increases the natural frequency. This phenomenon is due to the non-linear interaction between the load and the crack, which cannot be predicted if the crack and the load are treated separately by a simple superposition procedure.

To highlight the interaction effect between the crack and the axial load on the first natural frequency of the system, the term $\Delta\beta_{co}$, defined by equation (16), is plotted versus the axial load (U) for different crack depths (D) in Figure 4(b). This term is referred to as the coupling term. It represents the deviation in the value of $\Delta\beta_{DP}$ predicted by a superposition procedure from the value of $\Delta\beta_{DP}$ computed by the present model that takes into consideration the coupling effects between the crack and load. It is worth mentioning that the superposition method addressed above treats the effect of the crack and the effect of the load separately as follows:

$$\Delta\beta_{DP} = \Delta\beta_D + \Delta\beta_P. \tag{17}$$

From Figure 4(b) it can be seen that $\Delta\beta_{co}$ is equal to zero if either the load or the crack depth is zero. This result is also obvious from equation (14). Moreover, the figure shows that for small crack depth ($D \leqslant 0{\cdot}2$) and a wide range of axial load ($-50 \leqslant U \leqslant 30$), the coupling term is less than 1·0%. In other words, the error in computing $\Delta\beta_{DP}$ does not exceed 1·0% if the superposition procedure is used when the crack depth is less than 0·2. The coupling term is approximately a linear function of the load for small cracks (less than 0·2), though for a large crack depth $\Delta\beta_{co}$ is a non-linear function of the load.

The previous discussion is related to the behaviour of the first natural frequency of the system. The second natural frequency exhibits no change due to crack as mentioned earlier. Figure 6(a) shows that the third natural frequency is directly proportional to the tensile axial load, and it is inversely proportional to the compressive load. The effect of the axial load on the natural frequency can be considered linear for any value of crack depth without lack of accuracy. This result is shown clearly in Figure 7(b), where the partial derivative of the change in the natural frequency with respect to axial load ($\partial\Delta\beta_{DP}/\Delta U|_{D\text{-const.}}$) is plotted versus the load for different values of crack depths. This figure shows that ($\partial\Delta\beta_{DP}/\partial U|_{D\text{-const.}}$) has very small variation with respect to U for any value of D, and hence it can be considered as constant. The value of ($\partial\Delta\beta_{DP}/\partial U|_{D\text{-const.}}$) is very small. This gives an indication that the change in the third natural frequency is a slowly varying function of the load, for the given load range. On the other hand, the crack depth has a significant effect on $\Delta\beta_{DP}$, and the effect increases with increasing crack depth. This is clear from Figures 6(a) and 7(a). The latter shows the gradient of ($\Delta\beta_{DP}$) with respect to crack depth (D) ($\partial\Delta\beta_{DP}/\partial D|_{U\text{-const.}}$) versus axial load for different values of (D). For the range of load shown this gradient is negative, and therefore the third natural frequency is reduced by increasing the crack depth. However, the gradient with respect to D moves towards a positive value if the load moves towards compression. This phenomenon is noticed in the behaviour of the first natural frequency, as shown in Figure 5(a). The coupling term in the third natural frequency is shown in Figure 6(b). It is noticed that the coupling term is linear with respect to axial load for any value of crack depth. Also, the figure shows that for a wide range of crack depth ($D \leqslant 0{\cdot}50$ and axial load ($-50 \leqslant U \leqslant 30$), the absolute value of the coupling term is less than 1·5%. Thus, the superposition procedure gives good accuracy in determining the change in the third natural frequency due to crack and load. Comparison between the first and the third modes shows that the sensitivity of the first mode to crack and load is higher than the sensitivity of the third mode. Moreover, the variation of the first natural frequency versus loading is non-linear, but for the third mode this variation can be considered linear with good accuracy. Also, the same behaviour is noticed for the coupling term.

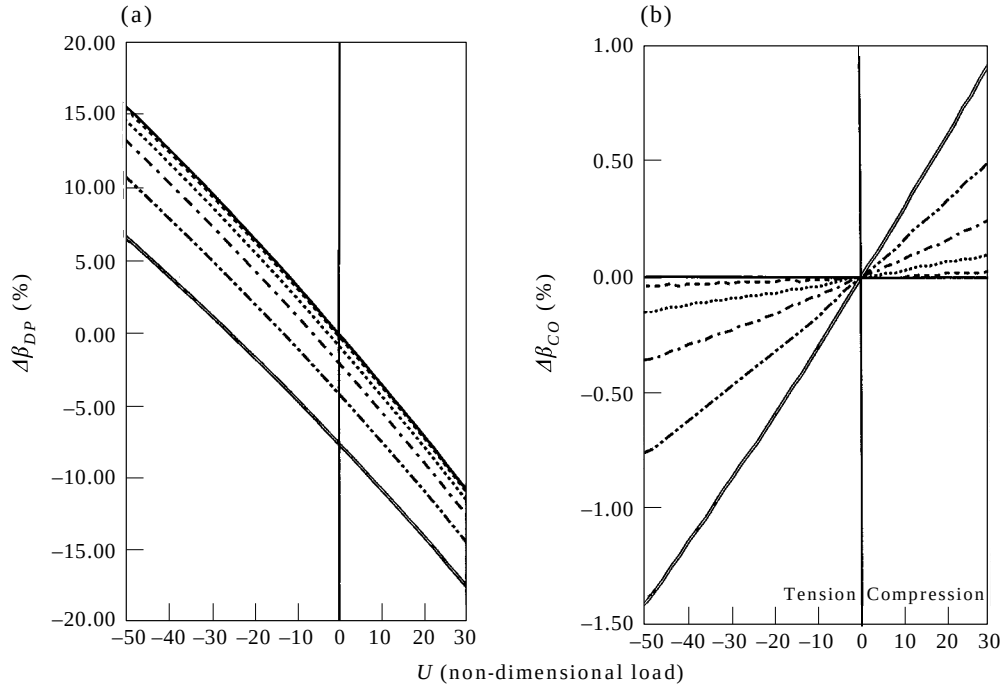

Figure 6. As Figure 4 but for third natural frequency.

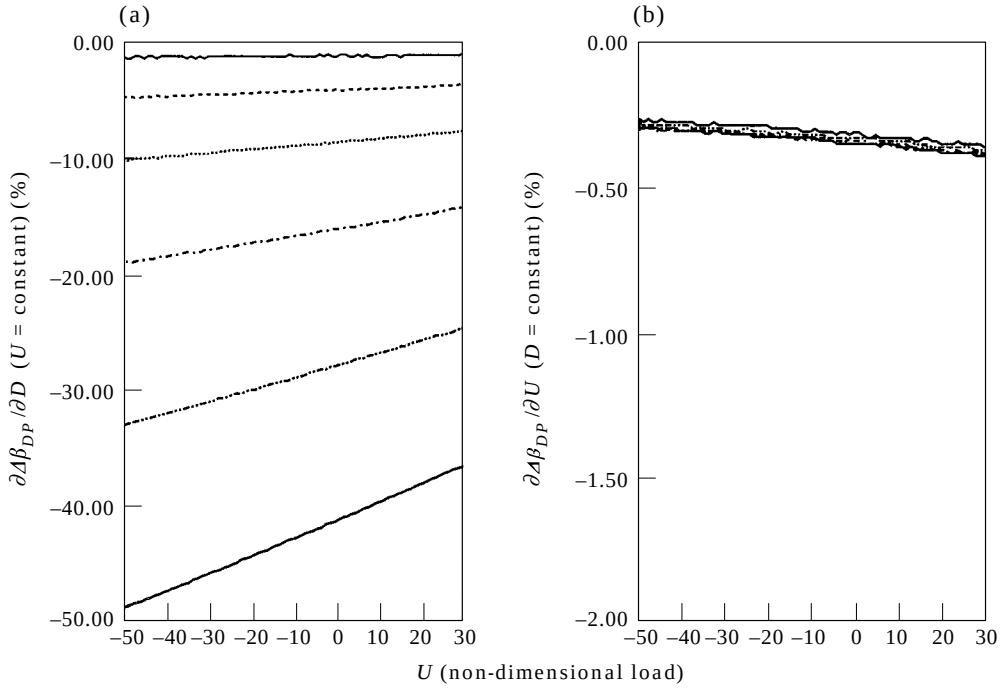

Figure 7. As Figure 5 but for third natural frequency.

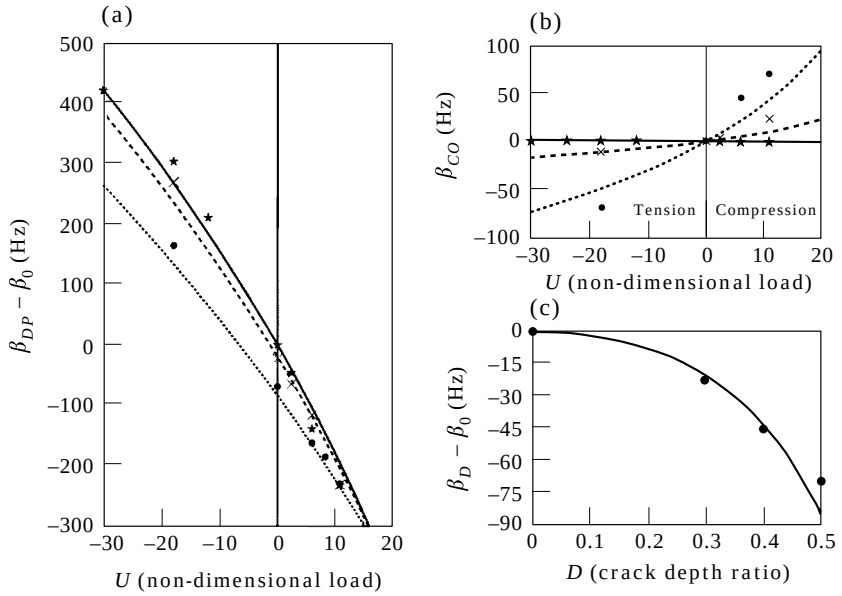

Figure 8. Change in the first natural frequency versus axial load for several crack depths; experimental and theoretical results. (a) Crack–loaded term; (b) crack–loaded coupling term; (c) crack–unloaded term; ●, experimental; ——, theoretical. Crack depth (D): ☆, 0·0 experimental; ×, 0·3 experimental; ●, 0·5 experimental; —, 0·0 theoretical; ——, 0·3 theoretical; · · · ·, 0·5 theoretical.

Finally, experimental work was carried out to verify the theoretical results. The verification was done for the first mode, and the results are shown in Figure 8. Figure 8(a) shows the changes in the first natural frequency for different values of load and crack. Since the mathematical model does not account for the weight of the accelerometers which is 8% of the beam's weight, the experimental measured frequency is expected to be less than the theoretical computed one. Therefore, the change in the frequency is presented as a difference between the cracked loaded case and the uncracked unloaded case in Hertz. In this way the shift in the experimental results (due to the accelerometer's weight) is eliminated. Consequently, a comparison between the experimental frequency change and the theoretical one can be carried out. The theoretical and experimental changes in the first natural frequency are plotted versus the axial load for different values of crack depth in Figure 8(a). By examining this figure, it can be seen that the experimental and theoretical results are in full agreement; similar agreement is seen in Figures 8(b) and (c). The coupling term versus the axial load for different crack depths is shown in Figure 8(b). This figure verifies the existence of the coupling term experimentally. Also, it can be seen that the proposed mathematical model is capable of predicting the behaviour of this term versus axial load and crack depth. Figure 8(c) presents the change in the first natural frequency for the unloaded beam versus crack depth. There is reasonable agreement between experimental and theoretical results, but, on the other hand, there is some deviation. This deviation is expected to be related to different sources. The first source is due to the assumption that the concentrated mass (accelerometer mass) is assumed to have a constant effect on the beam natural frequency independent of crack depth and load value. The second source is expected to be related to the assumption of rigid supports in the theoretical model, which is difficult to achieve experimentally. However, from Figure 8, it can be observed that the proposed theoretical model is capable of predicting the behaviour of the changes in the natural frequency of axially loaded cracked beams.

5. CONCLUSIONS

Investigation of the load–crack coupling of a fixed–fixed beam has been carried out theoretically and verified experimentally. The change in the natural frequency is obtained as a function of the crack depth and the axial load for the first three modes. The second mode is found to be insensitive to the crack depth. This result is expected for the second mode because the crack is located at the mid-span of the beam which is where a node is located. The following conclusions can be drawn from the present study.

(1) The effect of the load–crack coupling term is significant on the first mode compared to the third mode. The crack–load coupling behaviour of the first mode is highly non-linear. However, the coupling term in the case of the third mode is approximately linear. Both modes are affected asymmetrically by the load: i.e., in tensile loading, the crack coupling term reduces the natural frequency, while for compressive loading the crack coupling term increases the natural frequency. (2) For small crack depth and a wide range of loading, the change in the first natural frequency of the cracked loaded beam can be approximated by using a linear superposition between the effect of the crack and the effect of the load separately as follows: $\Delta\beta_{DP} = \Delta\beta_D + \Delta\beta_P$. The resultant error in this case is expected to be very small. However, for large crack depths the linear superposition leads to higher error. (3) For a crack depth up to 0·5 and a wide range of axial loading, the change in the third natural frequency can be predicted by using a linear superposition of the crack effect and the load effect separately. This superposition is expected to give an absolute error less then 1·5%. (4) The theoretical behaviour of frequency change versus load and crack has been verified experimentally.

REFERENCES

1. M. Biswas and A. K. Pandey 1989 *The International Journal of Analytical and Experimental Modal Analysis* **5**, 33–42. Diagnostic experimental spectral-modal analysis of a highway bridge.
2. T. G. Chondros and A. D. Dimarogonas 1980 *Journal of Sound and Vibration* **69**, 531–538. Identification of crack in welded joints of complex structures.
3. S. Christides and A. D. S. Barr 1984 *International Journal of the Mechanical Sciences* **26**, 639–648. One-dimensional theory of cracked Bernoulli–Euler beams.
4. E. H. Dannanh and S. H. Farghaly 1994 *Journal of Sound and Vibration* **170**, 607–620. Natural vibrations of cracked shafts carrying elastically mounted end mass.
5. C. A. Papadopoulos and A. D. Dimarogonas 1988 *Transactions of the ASME*, *Journal of Vibration*, *Acoustics*, *Stress*, *and Reliability in Design* **110**, 1–8. Coupled longitudinal and binding vibrations of a cracked shafts.
6. P. F. Rizos, N. Aspragathos and A. D. Dimarogonas 1990 *Journal of Sound and Vibration* **138**, 381–388. Identification of crack location and magnitude in a cantilever beam from the vibration modes.
7. Y. Narkis 1994 *Journal of Sound and Vibration* **172**, 549–558. Identification of crack location in vibrating simply supported beams.
8. B. S. Haisty and W. T. Springer 1988 *Transactions of the ASME*, *Journal of Vibration*, *Acoustics*, *Stress and Reliability in Design* **110**, 389–394. A general beam element for use in damage assessment of complex structures.
9. T. G. Gounaris and A. D. Dimarogonas 1988 *Journal of Computers and Structure* **28**, 309–313. A finite element of a cracked prismatic beam for structural analysis.
10. A. S. Sekhar and B. S. Prabhu 1994 *Journal of Sound and Vibration* **169**, 655–667. Vibration and stress fluctuation in cracked shafts.
11. T. G. Chondros and A. D. Dimarogonas 1989 *Journal of Vibration*, *Acoustics*, *Stress*, *and Reliability in Design* **111**, 251–256. Dynamic sensitivity of structures to cracks.
12. W. M. Ostachowicz and M. Krawczuk 1990 *Journal of Computers and Structures* **36**, 245–250. Vibration analysis of a cracked beam.
13. A. K. Pandey and M. Biswas 1994 *Journal of Sound and Vibration* **169**, 3–17. Damage detection in structures using change in flexibility.

14. M. H. H. Shen and C. Pierre 1990 *Journal of Sound and Vibration* **138**, 115–134. Natural modes of Bernoulli–Euler beams with symmetric cracks.
15. A. Bokaian 1988 *Journal of Sound and Vibration* **126**, 49–65. Natural frequencies of beams under compressive axial loads.
16. I. G. Currie and W. L. Gleghorn 1988 *Journal of Sound and Vibration* **123**, 55–61. Free lateral vibrations of a beam under tension with a concentrated mass at the mid-point.

APPENDIX: NOMENCLATURE

A	cross-sectional area of the beam
a	crack depth
D	crack depth ratio ($D = a/H$)
E	modulus of elasticity of the beam
H	half depth of the beam
I	area moment of inertia for the beam cross-section
L	total length of the beam
P	axial load (positive for compression, negative for tension)
t	time
U	non-dimensional load ($U = PL^2/EI$)
x	distance along beam axis
y	transverse deflection
β	non-dimensional frequency $\beta = \omega\sqrt{\rho AL^4/EI}$
$\Delta\beta_{DP}$	$= (\beta_{(crack\text{–}loaded)} - \beta_{(uncrack\text{–}unloaded)})/\beta_{(uncrack\text{–}unloaded)}$
$\Delta\beta_{P}$	$= (\beta_{(uncrack\text{–}loaded)} - \beta_{(uncrack\text{–}unloaded)})/\beta_{(uncrack\text{–}unloaded)}$
$\Delta\beta_{D}$	$= (\beta_{(crack\text{–}unloaded)} - \beta_{(uncrack\text{–}unloaded)})/\beta_{(uncrack\text{–}unloaded)}$
$\Delta\beta_{co}$	$= \Delta\beta_{DP} - \Delta\beta_{P} - \Delta\beta_{D}$
Θ	crack flexibility
η	x/L
ρ	mass density of the beam